ELSEVIER

Journal of Alloys and Compounds 253–254 (1997) 128–133

Journal of ALLOYS AND COMPOUNDS

Desorption characteristics of rare earth (R) hydrides (R=Y, Ce, Pr, Nd, Sm, Gd and Tb) in relation to the HDDR behaviour of R–Fe-based-compounds

V.A. Yartys[a,*], O. Gutfleisch[b], V.V. Panasyuk[a], I.R. Harris[b]

[a]Physico–Mechanical Institute of the National Academy of Sciences of Ukraine, 5, Naukova Str., Lviv, 290601, Ukraine
[b]School of Metallurgy and Materials, The University of Birmingham, Edgbaston, Birmingham, B15 2TT, UK

Abstract

Vacuum desorption characteristics of binary hydrides of rare earth metals (R=Ce, Pr, Nd, Y, Sm, Gd, Tb) were studied. A complete decomposition of hydrides, confirmed by X-ray diffraction, was achieved at temperatures up to 820 °C. When heating the hydrogenated material in vacuum, two distinct hydrogen desorption events were observed for all the hydrides under investigation. The hydrogen desorption behaviour is different for the two groups of metals, namely group I (Ce, Pr and Nd) and group II (Y, Sm, Gd and Tb). The hydrogenation–disproportionation–desorption–recombination (HDDR) process was shown to take place for the $Nd_6Fe_{13}Ge$ and $Nd_6Fe_{12.8}Ga_{1.2}$ intermetallic compounds, both with the $Nd_6Fe_{13}Si$-type structure. The hydrogen absorption and desorption properties of these compounds were studied in relation to the desorption characteristics of neodymium hydride.

Keywords: Rare earth metals; Hydrides; Desorption; HDDR

---

1. Introduction

The hydrogenation–disproportionation–desorption–recombination (HDDR) process has been applied very successfully to the production of magnetically coercive powders of $Nd_2Fe_{14}B$ [1,2] and $Sm_2Fe_{17}N_3$ [3]. In order to understand the HDDR process and to apply it to different rare earth systems, it is essential to characterise the stability and absorption and desorption behaviours of the particular R–hydrides. Phase equilibria in the binary systems of rare earth metals with hydrogen have been studied in a number of works (see, for example, [4–6]). For Ce, Pr and Nd the binary hydride covers the approximate range RH_2 to RH_3 whilst maintaining the face-centred cubic structure [7]. In contrast, a transformation from a cubic into a hexagonal crystal symmetry takes place on transition from the di-hydride to the tri-hydride for R=Y and rare earth metals Sm, Gd and Tb [7]. Measurements of hydrogen desorption isotherms indicated that, in a temperature range up to 1000 °C the plateaux of H_2 pressure on the P–C–T diagram for the RH_2–R systems are far below atmospheric pressure [5]. Vacuum desorption properties were studied in details only for neodymium hydride where a two-step decomposition was observed by mass-spectrometer studies at temperatures up to 800 °C [8]. In order to proceed with the recombination step of the HDDR route [1,2], two experimental procedures can be applied. First, a continuous hydrogen vacuum desorption at pressures below the equilibrium pressure on heating (up to 1000 °C), or secondly, application of a high temperature regime (above 1000 °C) where a substantial increase of the desorption equilibrium pressure will ensure the complete removal of hydrogen from the metal matrix, even under a hydrogen atmosphere. In the present work, vacuum desorption behaviours were determined for a number of $RH_{\sim 3}$ binary hydrides including R=Y, Ce, Pr, Nd, Sm, Gd and Tb. The HDDR routes for the compounds $Nd_6Fe_{13}Ge$ and $Nd_6Fe_{12.8}Ga_{1.2}$, both forming neodymium hydride on disproportionation, were also studied and are discussed in relation to the vacuum desorption behaviour of $NdH_{\sim 3}$.

2. Experimental details

The hydrides studied in the present work were obtained from the initial rare earth metals by heating them in

---

[*] Corresponding author. Fax: + 380 322 649427; e-mail: yartys@ah.ipm.lviv.ua

0925-8388/97/$17.00
PII S0925-8388(96)03097-6

hydrogen in a hydrogen DTA (HDTA) chamber. The sample chamber containing the rare earth metal sample with an average weight of 60–80 mg, was evacuated, filled subsequently with hydrogen (1 bar pressure) and then heated from room temperature with a rate of 5 °C min^{-1}. On heating, a strong exothermic reaction was observed indicative of hydride formation. The hydrogenation treatment lasted 15–30 min and was, in all cases, completed at temperatures below 500 °C. The hydrogen desorption properties of the hydrides were studied by cooling the material to room temperature and then evacuating the chamber. In this manner, the risk of oxidising the material was reduced significantly.

Subsequently, the material was heated at 5 °C min^{-1} and the temperature eventually increased to 800–850 °C, providing the conditions necessary for a complete desorption of the hydrides. The experimental details of the HDTA technique have been reported previously [9]. Temperature pressure analysis (TPA) was also performed [10], again using an initial hydrogen pressure of 1 bar and a heating rate of 5 °C min^{-1}.

The compounds, $Nd_6Fe_{13}Ge$ and $Nd_6Fe_{12.8}Ga_{1.2}$ were prepared by argon arc melting mixtures of the high purity constituent elements, with a subsequent annealing at 600 °C for 6 weeks in an attempt to homogenise the alloys. X-ray diffraction studies were performed with a Phillips PW 1012/10 diffractometer using Cu Kα radiation. Cell parameters were calculated using the least square refinement program LATTIC.

3. Results and discussion

3.1. $RH_{\sim 3}$ hydrides

The strongly exothermic behaviour of hydride formation causes a pronounced temperature increase accompanying hydrogenation (e.g. $\Delta T = 65$ °C in the case of Nd). A typical example is presented in Fig. 1 showing the data for Y. The hydrogenation was completed in the temperature range from 270 °C (Pr) to 455 °C (Tb). Saturated hydrides of rare earth metals belonging to group I (Ce, Pr and Nd) were formed at lower temperatures compared with those of group II (Y, Sm, Gd and Tb). As can be seen from the data presented in Table 1, the decomposition of hydrides proceeds over a wide temperature range from 100 °C (SmH_{3-x}) to 820 °C (YH_2). The measurements showed the existence of two separate events of hydrogen desorption for all the hydrides (see Fig. 2a–g). These events are associated with the low temperature desorption $RH_3 \rightarrow RH_2$ (approximate formulae) and the high temperature desorption $RH_2 \rightarrow R$. A clear difference in stability, both for the tri- and di-hydrides, was indicated for the two groups. In the case of the tri-hydrides of group I, the low temperature $RH_3 \rightarrow RH_2$ desorption consisted of two overlapping desorption events. A peak of hydrogen desorption observed at 340–380 °C, is preceded at lower temperatures by a shoulder in the hydrogen pressure curve. The most pronounced effects were observed for Pr which exhibited two low temperature peaks. The main desorption takes place at 340 °C and a smaller but clearly indicated second peak can be observed at 255 °C. In contrast, the low temperature desorption of the group II metals consisted of a regular, single-peak with an approximate Gaussian-type distribution. Consequently, the tri-hydrides of group II desorb over significantly narrower temperature ranges (160 °C for Y, 180 °C for Gd and 170 °C for Tb) compared to those of group I (230 °C for Nd, 270 °C for Pr).

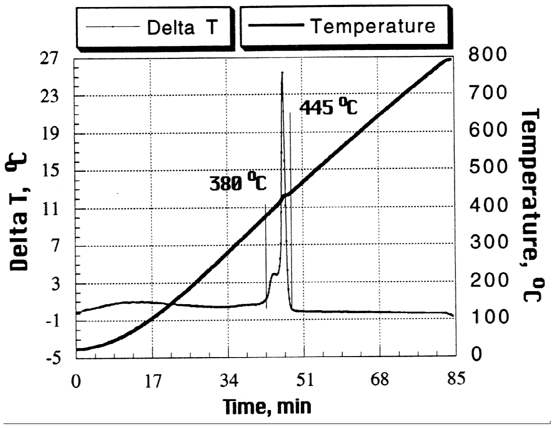

Fig. 1. Hydrogenation of yttrium in the HDTA rig (initial H_2 pressure 1 bar; heating rate 5 °C min^{-1}). Hydrogen absorption starts at 380 °C and is completed by 445 °C.

3.2. $RH_{\sim 2}$ hydrides

It can be seen from the data presented in Table 1 that, with increasing atomic number from Ce to Tb, the position of the high temperature peak rises gradually from 650 °C for Ce to 750 °C for Tb. The highest stability of di-hydride was observed in the case of the $YH_{\sim 2}$ (desorption peak at 790 °C). The eventual formation of the initial R metals

Table 1
Vacuum desorption behaviour of rare earth hydrides

Phase transition	Start	Peak	Finish
YH_3–YH_2	170	260	330
YH_2–Y	650	790	820
CeH_3–CeH_2	150	340	400
CeH_2–Ce	500	650	730
PrH_3–PrH_2	150	340	420
PrH_2–Pr	540	675	730
NdH_3–NdH_2	220	380	450
NdH_2–Nd	550	720	800
SmH_3–SmH_2	100	235	370
SmH_2–Sm	550	740	800
GdH_3–GdH_2	170	275	350
GdH_2–Gd	550	720	800
TbH_3–TbH_2	150	255	320
TbH_2–Tb	620	750	800

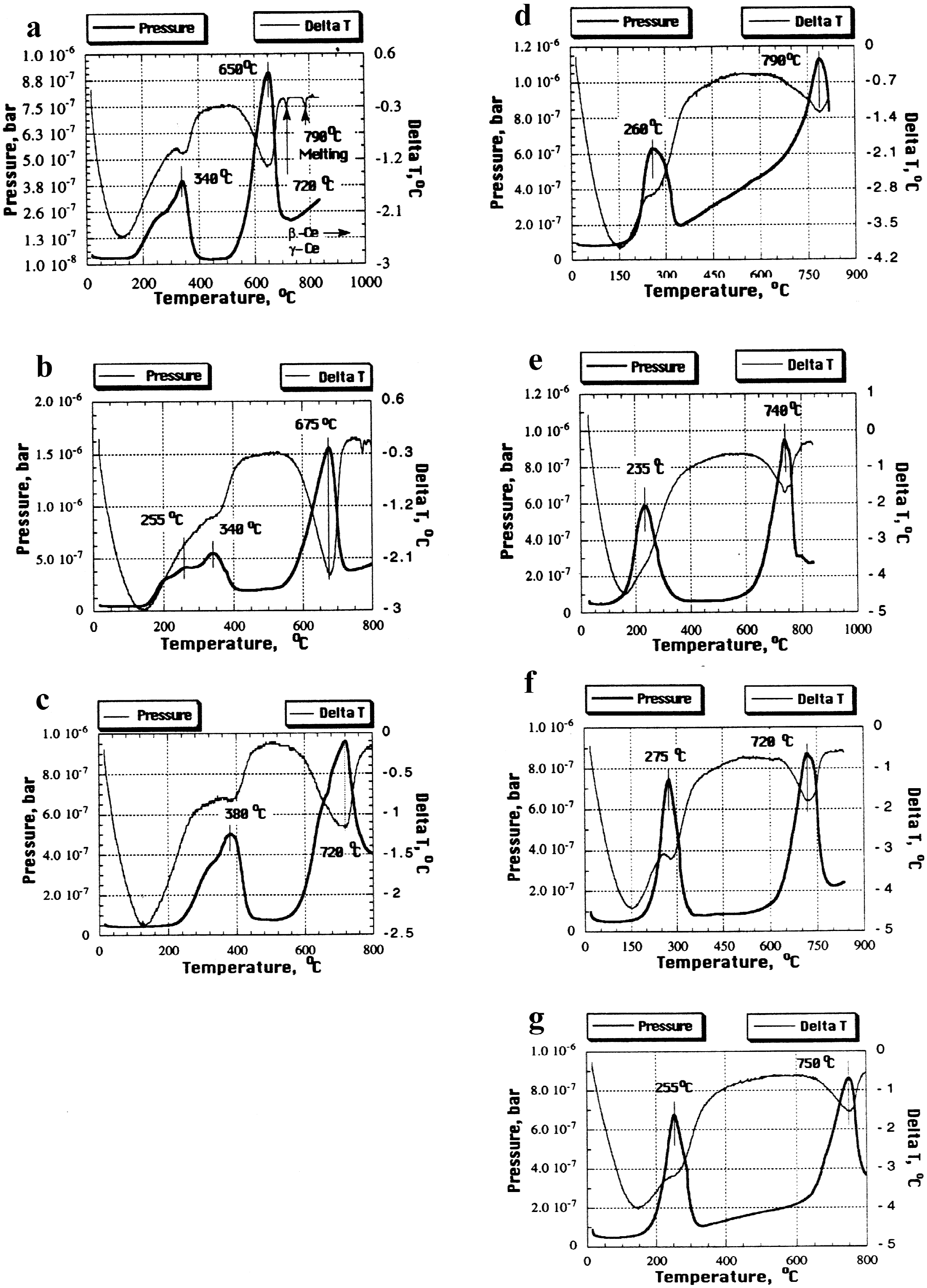

Fig. 2. HDTA traces of hydrogen desorption from the RH$_{\sim3}$ hydrides: (a) CeH$_{\sim3}$ (an allotropic transformation β-Ce–γ-Ce and melting of Ce are indicated on the DTA curve at 720°C and 790°C, respectively, above the temperature of complete hydrogen desorption); (b) PrH$_{\sim3}$; (c) NdH$_{\sim3}$; (d) YH$_{\sim3}$; (e) SmH$_{\sim3}$; (f) GdH$_{\sim3}$; (g) TbH$_{\sim3}$.

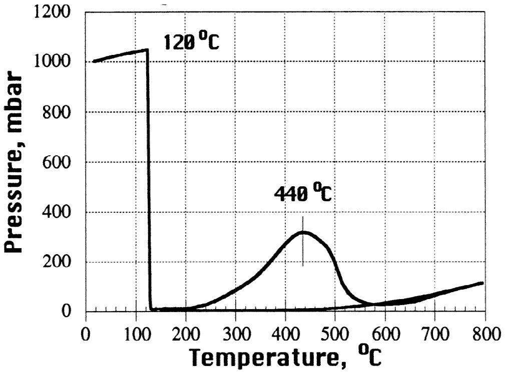

Fig. 3. TPA traces of hydrogen absorption for $Nd_6Fe_{12.8}Ga_{1.2}$ intermetallic compound.

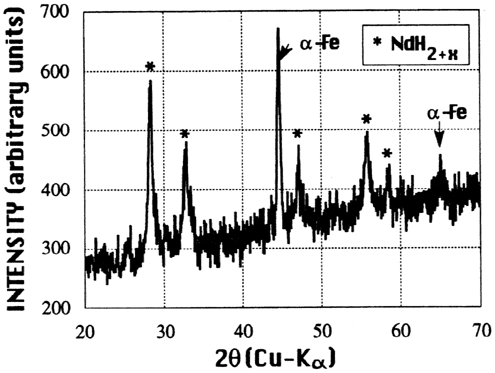

Fig. 4. XRD patterns for $Nd_6Fe_{13}GeH_x$ hydride after decomposition in the TPA chamber (heating in hydrogen up to 800 °C).

after hydrogen desorption was confirmed by X-ray diffraction. For example, the cell parameters of the hexagonal unit cells of Tb and Gd, after desorption, were found to be Tb: a=3.603(1) Å; c=5.682(4) Å and Gd: a=3.622(1) Å; c=5.772(4) Å. These results are in good agreement with the reference data for Tb (a=3.59 Å; c=5.66 Å) and Gd (a=3.63 Å; c=5.79 Å) metals [11].

3.3. HDDR behaviour of $Nd_6Fe_{13}Ge$ and $Nd_6Fe_{12.8}Ga_{1.2}$

In addition to η-$Nd_{1.1}Fe_4B_4$, $(Nd,Pr)_6Fe_{13}T$ (T-doping element) compounds can be formed as grain boundary phases when doping elements are added to (Nd,Pr)FeB permanent magnet alloy, as observed in the case of a $Pr_{17}Fe_{76}B_{5.5}Cu_{1.5}$ magnet [12]. $Nd_2Fe_{14}B_2$, (Φ-phase), and the ternary B-rich compounds in the Nd–Fe–B system, namely the η- and ρ-borides, all disproportionate in hydrogen on heating to 800 °C [13,14]. These processes were found to be reversible ($Nd_2Fe_{14}B$ [1,2], $Nd_5Fe_2B_6$ [14]) or irreversible ($Nd_{1.1}Fe_4B_4$ [13], (probably due to oxidation)). For the $R_6Fe_{13}T$ (R=Pr, Nd; T=Cu, Sb, Bi) compounds, studies of their hydrogenation properties have been limited to a temperature range of up to 350 °C [15]. At these temperatures no signs of a disproportionation reaction were observed.

In the present work, hydrogen absorption and desorption behaviour of $Nd_6Fe_{13}Ge$ and $Nd_6Fe_{12.8}Ga_{1.2}$ were investigated at temperatures up to 800 °C. X-ray diffraction studies and SEM investigations showed that both annealed alloys contained $Nd_6Fe_{13}Si$-type compounds as the main constituents, with small amounts of Nd-rich phase and Nd–Ge (Nd–Ga) binary compounds. TPA studies of the hydrogen absorption behaviour revealed two major absorption events for both compounds (see Fig. 3 where the data for $Nd_6Fe_{12.8}Ga_{1.2}$ are presented). The first absorption started at 120 °C ($Nd_6Fe_{12.8}Ga_{1.2}$) or 150 °C ($Nd_6Fe_{12.8}Ge$) and corresponds to the formation of $Nd_6Fe_{12.8}Ga_{1.2}H_{20.2}$ and $Nd_6Fe_{12.8}GeH_{18.5}$ hydrides. This absorption leads to the insertion of hydrogen atoms into the tetragonal unit cells of the compounds. Such insertion does not change their tetragonal symmetry. However, due to an anisotropic expansion of the cells in the [001] direction, the c/a ratio increased on hydrogen absorption from the initial values of 2.833 (Ga) and 2.851 (Ge) to a value of 3.116 (the latter was the same for both hydrides). The crystallographic characteristics of the intermetallic compounds and their hydrides are presented in Table 2.

On further heating, a second hydrogen absorption event was observed at 425 °C and 440 °C, respectively, for the Ge- and Ga-containing compounds. As indicated by XRD studies, this effect is associated with the decomposition of the metal matrix with the formation of NdH_{3-x} binary hydride and α-Fe as the main decomposition products (Fig. 4). Hydrogen desorption studies indicated clearly the nature of the hydrogenated material (insertion-type tetragonal hydride in the low temperature region or NdH_{3-x}-containing material on exposure of the alloy to hydrogen at temperatures up to 800 °C). For the saturated low temperature $Nd_6Fe_{13}GeH_{18.5}$ hydride, the desorption is completed

Table 2

Crystallographic characteristics of $Nd_6Fe_{13}Ge$ and $Nd_6Fe_{12.8}Ga_{1.8}$ intermetallic compounds and their hydrides

Compound/hydride	a (Å)	c (Å)	c/a	V (Å^3)	$\Delta a/a$ (%)	$\Delta c/c$ (%)	$\Delta V/V$ (%)
$Nd_6Fe_{13}Ge$	8.030(10)	22.89(4)	2.851	1476.0	–	–	–
$Nd_6Fe_{13}GeH_{18.5}$	8.111(3)	25.27(1)	3.116	1662.5	1.0	10.4	12.6
$Nd_6Fe_{12.8}Ga_{1.2}$	8.056(6)	22.82(2)	2.833	1481.0	–	–	–
$Nd_6Fe_{13}GaH_{20.2}$	8.178(6)	25.48(3)	3.116	1704.1	1.5	11.7	15.1

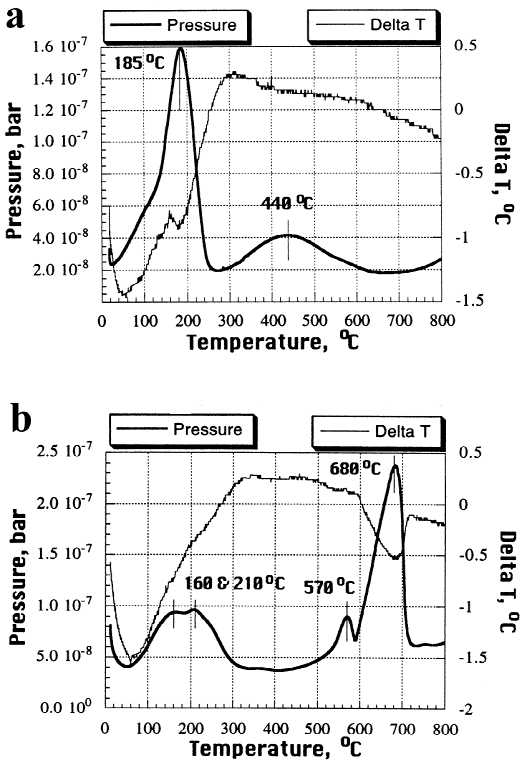

Fig. 5. HDTA desorption spectra: (a) $Nd_6Fe_{13}GeH_{18.5}$ saturated hydride; (b) $Nd_6Fe_{13}GeH_x$ decomposed hydride.

at 500 °C (see Fig. 5a) with the main desorption taking place at 185 °C and another, much weaker one, at 440 °C. After this treatment, return to the crystal lattice of the initial compound was confirmed by X-ray diffraction. As expected, in the case of the disproportionated $Nd_6Fe_{12.8}GeH_x$ material (NdH_{3-x}+α-Fe), the main desorption events (peaks at 160–210 °C and 680 °C, see Fig. 5b for details) are very similar to those observed for the NdH_{3-x} hydride (Fig. 2c). In both materials the major part of hydrogen is removed in the high temperature region due to desorption of NdH_2 to Nd. XRD studies showed that, on hydrogen desorption, the tetragonal $Nd_6Fe_{13}Ge$ and $Nd_6Fe_{12.8}Ga_{1.2}$ compounds are restored, thus indicating that the HDDR route takes place for these compounds.

4. Conclusions

The general desorption behaviour of the fully hydrogenated rare earth metals (R=Ce, Pr, Nd, Y, Sm, Gd, Tb), when heated in a vacuum, consists of the initial desorption of hydrogen to form the $RH_{\sim 2}$ composition followed by the complete desorption at much higher temperatures to form the R metal. This results in two distinct desorption events and these cover a wide temperature range from 100 °C ($SmH_{\sim 3} \rightarrow Sm_{H\sim 2}$) to 820 °C ($YH_{\sim 2} \rightarrow Y$). In all cases, the formation of the R metals on desorption was confirmed by X-ray diffraction studies. The group I metals (Ce, Nd, Pr) exhibited a broad (two peak) desorption behaviour at low temperatures whereas the group II metals (Y, Sm, Gd, Tb) only exhibited a single peak. For the $RH_{\sim 2}$ phases an increased stability was observed with increasing atomic number of the R-component.

The HDDR route was established for $Nd_6Fe_{13}Ge$ and $Nd_6Fe_{12.8}Ga_{1.2}$. A disproportionation reaction in hydrogen atmosphere of these compounds at temperatures above 500 °C was followed by a recombination reaction on desorption at the same temperature. Desorption from the disproportionated mixture exhibited close similarity to that of NdH_{3-x}. $Nd_6Fe_{13}Ge$ and $Nd_6Fe_{12.8}Ga_{1.2}$ compounds represent a new example of R-containing materials where the HDDR technique can be applied in order to modify the microstructure of the initial alloys.

Acknowledgments

Dr. I. Bulyk, Mr. J. Clarke, Mr. A. Riabov, Mr. D. Willey and Dr. A.J. Williams are thanked for their invaluable help in the experimental work and in the preparation of the manuscript. The School of Metallurgy and Materials and the National Academy of Sciences of Ukraine are gratefully acknowledged for their support. The authors would like to thank the Royal Society for the provision of research grant supporting a collaborative research program between the PhMI NAS Ukraine and the School of Metallurgy and Materials, The University of Birmingham. This work was supported in part by ICF grant UCQ2OO.

References

[1] T. Takeshita and R. Nakayama, *Proc. 10th Int. Workshop on Rare Earth Magnets and their Applications*, Kyoto, 1989, p. 551.
[2] I.R. Harris, *Proc. 12th Int. Workshop on Rare-Earth Magnets and their Applications*, Canberra, 1992, p. 347.
[3] S. Sugimoto, H. Nakamura, M. Okada and M. Homma, *Proc. 12th Int. Workshop on Rare-Earth Magnets and Their Applications*, Canberra, 1992, p. 372.
[4] C.E. Messer and M.K. Park, *J. Less-Common Metals, 26* (1972) 235.
[5] C. Ohki, H. Uchida and E. Ko, *J. Japan Inst. Metals, 54* (1990) No. 2, 146.
[6] M.H. Mintz, Z. Hadari and M. Bixon, *J. Less-Common Metals, 37* (1974) 331.
[7] K.M. MacKay, *Hydrogen Compounds of the Metallic Elements*. E. and F.N. Spon, London, 1966.
[8] A.J. Williams, P.J. McGuiness and I.R. Harris, *J. Less-Common Metals, 171* (1991) 149.
[9] D. Book, I.R. Harris, A. Manaf, I. Ahmad and H.A. Davies, *J. Alloys Comp., 221* (1995) 180.
[10] D. Book and I.R. Harris *J. Alloys Comp., 221* (1995) 187.
[11] *Metals Reference Book*, C.I. Smithells (ed.), Butterworth, London and Boston, 1976.

[12] T. Kajitani, K. Nagayama and T. Umeda, *Proc. 12th Int. Workshop on RE Magnets and Their Applications*, Canberra, 1992, p. 574.

[13] V.A. Yartys, O. Gutfleisch and I.R. Harris, *J. Magn. Magn. Mater.*, *119* (1996) 157–158.

[14] V.A. Yartys, O. Gutfleisch and I.R. Harris, *J. Alloys Comp.*, *253–254* (1997) 134–139.

[15] J.M.D. Coey, Quinian Qi, K.G. Knoch, A. Leithe-Jasper and P. Rogl, *J. Magn. Magn. Mater.*, *129* (1994) 87.